

Nickel removal from aqueous solution by non-living *Pleurotus mutilus*: kinetic, equilibrium, and thermodynamic studies

N. Daoud, A.Selatnia*, E.H. Benyoussef

Laboratoire des Energies Fossiles. Ecole Nationale Polytechnique d'Alger. Département de Génie Chimique. 10, Avenue Pasteur. Belfort. EL-Harrach. Alger. Algeria

*Corresponding author: ammarselatnia@yahoo.fr; Tel: +213 5 52 48 55 67

ARTICLE INFO

Article History:

Received : 21/08/2018

Accepted : 20/10/2018

Key Words:

Bisorption;
Nickel(II);
Pleurotusmutilus;
Batch processing.

ABSTRACT/RESUME

Abstract: Fungal biomass is cost-efficient and efficient biosorbent for heavy metals removal. In this paper the ability of fungal biomass *Pleurotusmutilus* (filamentous fungi) to remove Ni(II) from aqueous solutions has been undertaken. The speciation of Ni(II) was modeled and the most probable precipitates forming were predicted using visual MINTEQ. The surface of fungal biomass was characterized by pH_{PZC} determination, and Boehm and potentiometric titrations. The effects of various physico-chemical factors on Ni(II) bisorption were investigated. The optimum pH for Ni(II) removal was achieved at pH 8.0. The maximum adsorption capacity calculated from Langmuir adsorption isotherm was 47.169 mg/g. The adsorption isotherms fitted the data in the order: Dubinin-Radushkevich>Temkin>Freundlich>Langmuir. The bisorption kinetic data were fitted well with the pseudo-second-order kinetic model. The negative values of Gibbs free energy (ΔG^0) indicate the feasible and spontaneous adsorption of nickel.

I. Introduction

Heavy metal pollution is one of the most important environmental issues today. Pollution by nickel usually comes from several industrial processes such as electroplating, mining, fertilizers, pigments [1], dyeing operation, leather tanning, paint formulation, ceramic and porcelain enameling industries [2]. The health hazards associated with Ni(II) include renal edema, lung cancer, pulmonary fibrosis, skin dermatitis, and gastro intestinal discomfort [3]. Hence, the treatment of nickel contaminated industrial effluents is necessary. The most widely used methods for removing Ni(II) from contaminated waters include chemical precipitation, ion-exchange, ion flotation, membrane filtration, adsorption and electrochemical treatment [4]. Nonetheless, these methods are not effective enough at low concentrations and are also very expensive as a result of high chemical reagent and energy requirements. They also have the major drawback of generating toxic secondary sludge [5]. In recent years, bisorption has emerged as a cost-efficient and effective alternative for the removal of nickel from wastewaters [2, 6]. A variety of microbial

systems have been used as biosorbents for nickel removal from wastewaters such as: bacteria [7], fungi [8] and algae [9]. Problems associated with metal toxicity in living biomass and the need to provide suitable growth condition also do not arise. Many early studies have shown that nonliving biomass may be even more effective than living cells in sequestering metallic elements [10]. A variety of biomass is used by the SAIDAL antibiotic complex at Medea, Algeria, among which the filamentous fungi (*Pleurotusmutilus*) is isolated. Huge quantities of fungal residue are produced from the antibiotic extraction process. The ability of *Pleurotusmutilus* to remove heavy metals [11-13], dye [14] and pesticide [15] has already been studied. However, to our knowledge, no study has been reported on the bisorption of nickel by *Pleurotus mutilus*. The main objective of this work was to study the Ni(II) adsorption using biomass of dead *Pleurotus mutilus*. The effect of four different factors and the mechanisms of bisorption were also studied. The parameters of the bisorption isotherms and kinetics were determined from bisorption measurements.

II. Materials and methods

II.1. Biosorbent Preparation

A residual biomass of non-living *Pleurotusmutilus* filamentous fungi biomass, produced during veterinary antibiotic pleuromutiline production, was obtained from SAIDAL antibiotoxic complex (Medea, Algeria). The biomass was washed with distilled water and dried at 60°C for 24 h, then crushed and sieved to the desired particle size.

II.2. Biosorbent characterization

II.2.1. Determination of zero point charge

Zero point charge is the pH at which the external surface charge of a particle is zero, i.e. the number of positively charged centers is equal to the number of negatively charged centers [16]. The pH point of zero charge (pH_{zpc}) determination was carried out by adding 0.1 g of biomass to 50 mL solution of 0.01 M KNO₃ (1.01 g/L) whose initial pH has been measured and adjusted with HCl 0.1 M or NaOH 0.1 M solutions. The container was sealed and placed on a shaker for 48 h at room temperature before measuring the pH of the solution. The point of zero charge (pH_{zpc}) is the value at which the curve pH_{initial}-pH_{final} = f (pH_{initial}) intersects pH_{initial} axis [16, 17].

II.2.2. Boehm titration

Acidic and basic sites on the biosorbent were determined by the acid-base titration method proposed by Boehm [18]. Triplicate 0.5 g samples of the biomass were shaken with 50 mL solution of NaHCO₃ (0.1 M), Na₂CO₃ (0.05 M) and NaOH (0.1 M) for acidic groups and 0.1 M HCl for basic groups respectively at room temperature (24 ± 2°C) for 72 h in closed centrifuge tubes. The stock solution was prepared from analytical grade product (Merck, Darmstadt, Germany) in deionized water. The equilibrated Boehm reactants were separated from the biomass by filtration using 0.45 μm nitrocellulose filter paper. The isolated solution is acidified then boiled to remove CO₂. Finally, aliquots of the isolated solutions are back-titrated with a standardized NaOH solution to determine the quantity of the Boehm reactants that were neutralized during the initial equilibration with the solid. The numbers of the various acidic site types were calculated under the assumption that NaOH neutralizes carboxylic, phenolic and lactonic groups, Na₂CO₃ carboxylic and lactonic and NaHCO₃ only carboxylic groups. Lactones are assumed to be the difference between the groups titrated with Na₂CO₃ and those titrated with NaHCO₃ and phenols are assumed to be difference between the groups titrated with NaOH and those titrated with Na₂CO₃. The number of surface basic sites was calculated from the amount of hydrochloric acid which reacted with the biomass. Neutralization points were known using pH

indicators of phenolphthalein solution for titration (1 g of phenolphthalein in 100 mL of ethanol 95 %).

II.2.3. Potentiometric titration

Potentiometric titration was performed using an automatic microburette (Witeg, West Germany) and a hotplate stirrer (Stuart, heat-stir, SB 162). The pH glass electrode (pH-meter Jenway 3310) was calibrated with buffer solutions of pH 4.0, 7.0 and 9.0. The temperature is constant during the experiment (25°C). The titration cell was filled with 50 mL of 0.1 mol/L NaNO₃ solution (or 0.01 mol/L) and 0.15 g of biomass. Then, the suspension was acidified to pH 3.0, using 0.1 mol/L HCl solution under constant magnetic stirring (250 rpm). Titration was carried out by stepwise addition of 0.1 mL of 0.0134 mol/L NaOH. The suspension was bubbled for 30 min with N₂ to remove CO₂ and limit its dissolution. After NaOH addition, the drift rate was measured over time, and readings were accepted when the drift was less than 2 mV/min [19, 20]. Potentiometric titration can be performed to evaluate cation exchange capacity (CEC) of the biosorbent, i.e. the number of negatively charged sites per unit of biomass mass [21]. The calculation of cation exchange capacity (meq/g) was carried out using the following equation:

$$CEC = \frac{c(V-v)}{m} \quad (1)$$

where C (mmol/L) is the concentration of the NaOH solution added, V (L) is the volume of NaOH solution added to the biosorbent suspension at defined value of pH, v (L) is the volume of NaOH solution needed to reach the same pH in blank experiments (without biosorbent) and m (g) is the weight of biosorbent.

II.3. Speciation and saturation index (SI) calculation

The chemical equilibrium software, visual MINTEQ v 3.1 was used to predict nickel speciation depending on metal concentration and solution pH and calculate the saturation indices (SI).

The SI for a solid is defined as:

$$SI = \log \left(\frac{IAP}{K_s} \right) \quad (2)$$

IAP is the ion activity product and K_s is the temperature-corrected solubility constant.

Oversaturation is indicated if SI > 0, whereas the solution is undersaturated with respect to the solid if SI < 0. There is an apparent equilibrium with respect to the solid when SI = 0 [22].

II.4. Solution preparation

A stock solution of 1000 mg/L of Ni(II) was prepared from nickel standard solution (NiCl₂, Titrisol Merck) in deionized water. Other

concentrations varying between 50 and 500 mg/L were prepared from stock solution by dilution.

II. 5. Batch biosorption experiments

The biosorption tests were carried out in closed system. Batch experiments were executed in 250 mL Erlenmeyer flask, containing 100 mL solution of metal ions [23, 24]. A known amount of Ni(II) prepared with NiCl₂ salt was added to the suspended biomass in solution (3g/L) until adsorption equilibrium was reached. A magnetic stirrer was used to homogenize the mixture. The stirring speed of 250 rpm was used in all our experiments (IKA Labortechnik KS 250 basic) [25]. Each experiment was conducted three times in order to confirm the results. Ni(II) residual concentrations in solution were determined by Atomic Absorption Spectrophotometer with a wavelength of 232 nm. The initial pH of the solutions containing biomass was adjusted with HCl (0.1 M) and NaOH (0.1 M) solutions, with no significant dilution effect to defined values at initial time before adding nickel (pH Meter Jenway 3310). Experiments were conducted at room temperature (24 ± 2°C). Biosorption studies were done using various parameters such as time (2-120 min), pH (3.0-10.0), Ni(II) concentrations (50-500 mg/L), and particles size (50-100 µm, 100-200 µm, 200-300 µm).

The metal uptake q (mg/g) was calculated from the difference between initial concentration C_i (mg/L) and final equilibrium concentration C_f (mg/L) of the metal in solution according to the following equation:

$$q = \frac{V(C_i - C_f)}{m} \quad (3)$$

where V (L) is the liquid sample volume and m (g) is the starting sorbent weight.

II.6. Biosorption isotherms

Out of several isotherm equations, the Langmuir, Freundlich, Temkin, and Dubinin-Radushkevich (D-R) isotherm models were used to describe the equilibrium between adsorbed Ni(II) on fungal biosorbent and Ni(II) in solution.

II.6.1. Langmuir model

The Langmuir isotherm model is appropriate for the monolayer type sorption where all sites on the surface of the sorbent have the same affinity and assume no migration of metal ions in the surface sites. This model was chosen to estimate the maximum adsorption capacity corresponding to complete monolayer coverage on the biomass surface [26, 27]. The mathematical formula of the

linear form of Langmuir equation can be expressed as:

$$\frac{1}{q_e} = \frac{1}{q_{\max}} + \frac{1}{q_{\max} K_L C_e} \quad (4)$$

$$R_L = \frac{1}{1 + K_L C_0} \quad (5)$$

where, q_e (mg/g) is the amount of adsorbed nickel ions per unit weight of biomass and C_e (mg/L) is the unadsorbed nickel ions concentration in solution at equilibrium.

q_{\max} is the maximum amount of nickel ions per unit weight of biomass required to form a complete monolayer on the surface bound at high C_e (mg/g) and K_L (L/mg) is a constant that impacts the affinity of the binding sites. Another essential characteristics of the Langmuir isotherm can be described by the separation factor R_L (Eq. (5)) that reflects the biosorption process and is classified into unfavorable ($R_L > 1$), linear ($R_L = 1$), favorable ($0 < R_L < 1$) or irreversible ($R_L = 0$) [26].

II.6.2. Freundlich model

The Freundlich model describes adsorption to heterogeneous surfaces. It was chosen to estimate the adsorption intensity of the biosorbent towards the biomass [26, 27]. The linear form of this model is given by the equation (6):

$$\ln q_e = \frac{1}{n} \ln C_e + \ln K_f \quad (6)$$

Where q_e (mg/g) is the amount adsorbed at equilibrium and C_e is the equilibrium concentration of the adsorbate. K_f is the adsorption capacity and “ n ” the intensity of adsorption. The “ n ” parameter is known as heterogeneity factor and it has been used to evaluate whether the adsorption process is physical ($n > 1$), chemical ($n < 1$), or linear ($n = 1$) [28].

II.6.3. Temkin model

Temkin isotherm considers that the fall in the heat of sorption is linear rather than logarithmic, as implied in the Freundlich equation. The heat of sorption of all the molecules in the layer would decrease linearly with coverage due to sorbate/sorbent interactions [29, 30]. The Temkin isotherm has been used in the following linear form:

$$q_e = \frac{RT}{b_T} \ln a_T + \frac{RT}{b_T} \ln C_e \quad (7)$$

where q_e (mg/g) is the adsorbed amount at equilibrium and C_e (mg/L) the equilibrium concentration of the adsorbate, b_T (J/mol) is the

Temkin constant related to heat of sorption and a_T (L/mg) the equilibrium binding constant [29, 31].

II.6.4. Dubinin-Radushkevich (D-R) model

The Dubinin-Radushkevich (D-R) model does not assume a homogeneous surface or a constant biosorption potential as the Langmuir model. The mathematical formula of The Dubinin-Radushkevich (D-R) model is written as follows:

$$\ln q_e = \ln q_D - \beta \varepsilon^2 \quad (8)$$

Where q_D (mg/g) is the theoretical saturation capacity of the adsorbate retained, β is the activity coefficient related to mean sorption energy and ε , the Polanyi potential, which is equal to:

$$\varepsilon = RT \ln \left(1 + \frac{1}{C_e} \right) \quad (9)$$

where R (J/mol K) is the gas constant and T (K) is the absolute temperature.

The mean energy of sorption, E , can be calculated as follows:

$$E = \frac{1}{\sqrt{2\beta}} \quad (10)$$

If $E < 8000$ J/mol, the adsorption is dominated by physisorption, if E is between 8000 and 16000 J/mol, the adsorption process is dominated by chemisorption mechanism and if $E > 16000$ J/mol, the adsorption process is dominated by particle diffusion [32].

II.7. Biosorption kinetic models

Many kinetic models have been proposed to elucidate the mechanism of adsorption and its potential rate-controlling steps that include mass transport and chemical reaction processes. Several kinetic models such as pseudo-first-order, pseudo-second-order, Elovich, intraparticle diffusion and Boyd models were commonly used to test the experimental data.

II.7.1. Pseudo-first-order kinetic model

The pseudo-first-order kinetic model was proposed by Lagergren [33]. The integral form of the model was generally expressed as follows:

$$\log(q_e - q_t) = \log q_e - \frac{k_1}{2.303} t \quad (11)$$

where, q_e (mg/g) and q_t (mg/g) are the amounts of adsorbed Ni(II) on the adsorbent at equilibrium and at time t respectively and k_1 (min^{-1}) is the first-order rate constant.

II.7.2. Pseudo-second-order kinetics

The pseudo-second-order model is proposed by Ho and McKay [34] and based on the assumption that the adsorption follows second order

chemisorption. The linearized form of the pseudo-second-order model can be expressed as:

$$\frac{1}{q_t} = \frac{1}{k_2 q_e^2} + \frac{1}{q_e} t \quad (12)$$

Where k_2 (g/mg min) is the second order adsorption rate constant and q_e (mg/g) the adsorption capacity calculated by the pseudo-second-order kinetic model.

The constant k_2 is used to calculate the initial sorption rate h (mg/g min) at $t \rightarrow 0$ as follows [35]:

$$h = k_2 q_e^2 \quad (13)$$

II.7.3. Elovich model

The Elovich equation is valid for heterogeneous surfaces and mainly applicable for chemisorption process. The Elovich model can be written as [6]:

$$q_t = \frac{1}{\beta} \ln(\alpha\beta) + \frac{1}{\beta} \ln t \quad (14)$$

Where α (mg/g min) is the initial adsorption rate and β (mg/g min) Elovich constant related to the extent of surface coverage and also to the activation energy involved in chemisorption (g/mg).

II.7.4. Intra-particle diffusion model

During the biosorption process, the adsorbate transfer is characterized by boundary level diffusion and/or intraparticle diffusion. The intraparticle diffusion model assumes that the film diffusion is negligible and intraparticle diffusion is the only rate-controlling step, especially in a rapidly stirred batch reactor [36]. In order to investigate the adsorption is intra-particle diffusion or film diffusion, Weber and Morris [36] suggested the following kinetic model:

$$q_t = K_p t^{1/2} + C \quad (15)$$

Where k_p (mg/g $\text{min}^{1/2}$) is the intra-particle diffusion rate constant, q_t (mg/g) is the amount of Ni(II) adsorbed at time t and C (mg/g) is a constant related to the thickness of the boundary layer. If the adsorption process follows the intra-particle diffusion model, then q_t versus $t^{1/2}$ will be linear and if the plot passes through the origin, then the rate limiting process is the intraparticle diffusion.

II.7. 5. Boyd model

Due to both the film diffusion and the intraparticle diffusion, Boyd model is used to determine the actual rate-controlling step involved in the Ni(II) biosorption process. The kinetic data as obtained by the batch method were further analyzed using the Boyd model given by Boyd et al. [37]:

$$B_t = -0.4977 - \ln(1 - F) \quad (16)$$

$$F = \frac{q_t}{q_e} \quad (17)$$

where F (mg/g) is the amount of metal ions adsorbed at equilibrium, q_t (mg/g) represents the amount of ions adsorbed at anytime t (min). The linearity of the plots can be used to identify whether film diffusion or intraparticle diffusion controls the rate of Ni(II) sorption process. A straight line passing through the origin is indicative of biosorption processes governed by particle-diffusion mechanisms; otherwise, they are governed by film diffusion [38].

II.8. Thermodynamics of biosorption

The thermodynamics of Ni(II) sorption onto biomass of *Pleurotusmutilus* was evaluated using following equations:

$$K_c = \frac{C_{Ae}}{C_{Se}} \quad (18)$$

$$\Delta G^0 = -RT \ln K_c \quad (19)$$

Where K_c is the equilibrium constant, which is the ratio of the equilibrium concentration of nickel ions on the adsorbent to the equilibrium concentration of nickel ions in solution. R (8.314 J/mol.K) is the universal gas constant, T (K) is the absolute temperature.

II.7. Statistical analysis

All the experiments were performed in triplicates and the data represent the average of the values obtained. All data analyses were performed using an XLStat 7.5.2. The data were evaluated by ANOVA with significance set at $p < 0.05$.

III. Results and discussion

III.1. Characteristics of *Pleurotusmutilus*

III.1.1. The point of zero charge (pH_{zpc})

The zero point charge was found to occur at the pH of 7.94 as presented in figure. 1.

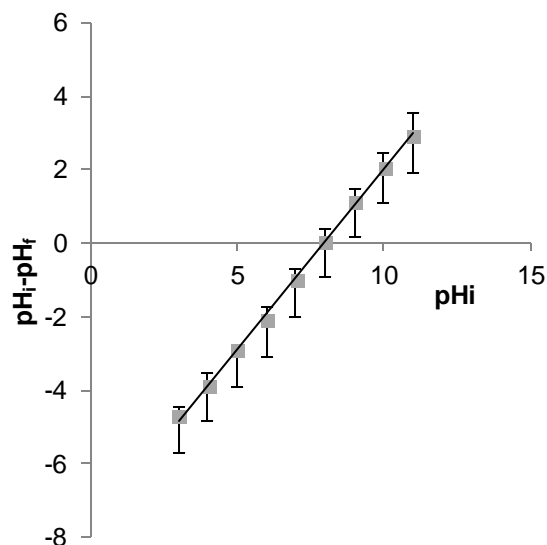


Figure 1. Determination of the zero point charge of *Pleurotusmutilus*.

The surface of *Pleurotusmutilus* will be negatively charged above the pH of 7.94 and positively charged below this pH value [39, 40].

III.1.2. Boehm titration

According to the experimental data obtained by Boehm method, the quantities of acidic sites matching the carboxylic, phenolic and lactonic sites [41] and basic sites for *Pleurotusmutilus* are presented in table 1.

Table 1. Functional groups determined by Boehm method.

Biomass	Acidic sites				Basic sites (meq/g)
	Total (meq/g)	Carboxylic (meq/g)	Phenolic (meq/g)	Lactonic (meq/g)	
<i>Pleurotus mutilus</i>	4.33	3.35	0.46	0.52	2.32

These results indicate that the surface of *Pleurotusmutilus* is acidic.

III.1.3. Potentiometric titration and Cationic Exchange Capacity

In order to gain closer insight of biomass surface properties, a suspension of biomass was potentiometrically titrated applying 0.1 M NaOH.

The results provided a rough characterization of the fungal biomass, since the ionic exchange is one of the prevalent mechanisms in the removal of Ni(II) from aqueous solution. The curve displayed on figure. 2 shows inflexion points which correspond to pK_a values of the binding functional groups. In fact, pK_a determines such pH, above which functional

groups of particular type are in the ionized form, capable of exchanging H^+ with metal cations from the solution [42].

An evaluation of the inflexion point is performed by searching for zero values of the second derivative of pH versus titrant volume, which correspond to maximum and minimum values of the first derivative. Table 2 shows the identified chemical binding groups with their pK_a , for two ionic forces.

Table 2. Functional groups and their pK_a on *Pleurotusmutilus* conditional on Ionic Strength at 0.01 and 0.1 M.

Functionalgroup	I = 0.01M	I = 0.1 M
Carboxyl	3.4, 3.88	3.62
Imidazole	5.55	5.64
Phosphate	6.8	6.88

The titration curve of *Pleurotusmutilus* (Figure. 2) showed inflexion points at pH 3.4, 3.88 and 5.5 for ionic strength of 0.01M and pH 3.62 and 5.64 for ionic strength of 0.1 M corresponding to carboxylic (pK_a 1.7-4.7) and imidazol (5.5-6) as acidic groups. The curve showed also one inflexion point at pH 6.8 for ionic strength of 0.01 M and 6.88 for ionic strength of 0.1 M corresponding to the alkaline functional group of phosphate (pK_a 6.1-6.8) as summarized in table 2 [43, 44].

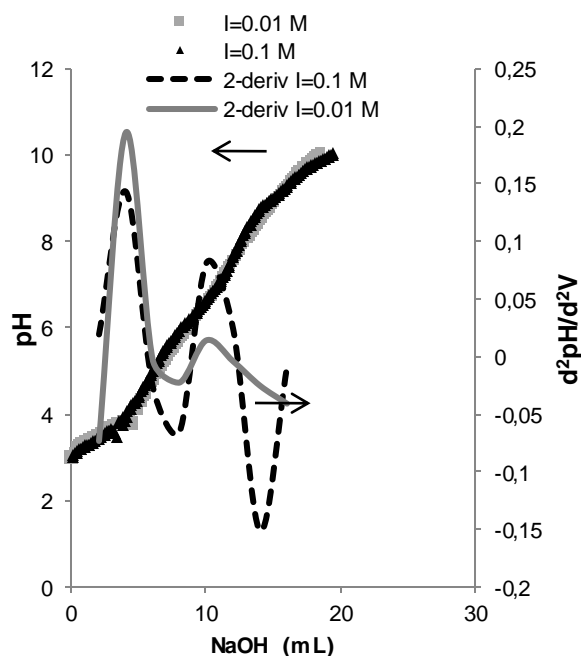


Figure2. Potentiometric titration curves and second derivative plots (2-deriv) of *Pleurotusmutilus* for ionic strengths $I = 0.01$ M and $I = 0.1$ M.

The pK_a values obtained for the ionic strength of 0.01 M are higher than the value obtained for ionic

strength of 0.1 M. These results were expected as an increase in ionic strength lowers most pK_a values [45].

FTIR analysis performed by Chergui et al. [11] on the *Pleurotusmutilus* biomass confirms the existence of Sulfonate groups. Potentiometric titration did not confirm involvement of these groups ($-SO_3^-$) in cation exchange, since it was performed in the range of pH 3.01-10.01. Sulfonate groups usually only contribute to metal binding at low pH, and their typical pK_a values are in the range of 1.0-2.5 [46].

The cationic exchange capacity (CEC) of *Pleurotusmutilus* was found to increase with increase in pH but does not change with ionic strength variation (Figure. 3).

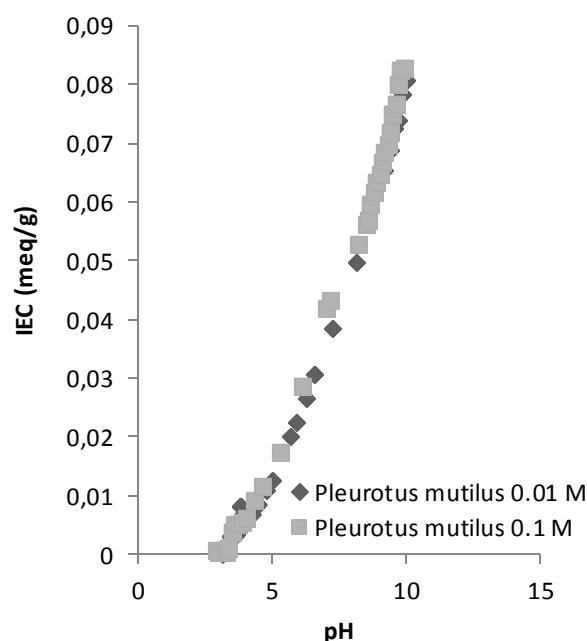


Figure3. Cation exchange capacity as function of pH for ionic strength of 0.1 M and ionic strength of 0.01 M.

III.2. Speciation and saturation index (SI)

Visual MINTEQ V 3.1 software was used to calculate the distribution of Ni(II) chemical species in the solution and the possibility of mineral precipitation at the concentration of 300 mg/L. The concentration of Ni(II) ions in the solution does not change significantly at pH values ranging from 3.0 to 8.0 as free metal ions mainly dominated in solutions. Then the concentration of Ni(II) decreases up to pH 10.0 as nickel precipitated mainly as $Ni(OH)_2$ (figure. 4). The calculations showed that at pH values higher than 7.14 the saturation index for $Ni(OH)_2$ was higher than 0. The saturation was significant only for pH values higher than 8.0.

On considering the pH_{pzc} and the precipitation of nickel as $Ni(OH)_2$, pH 8.0 was selected as optimum pH for Ni(II) adsorption.

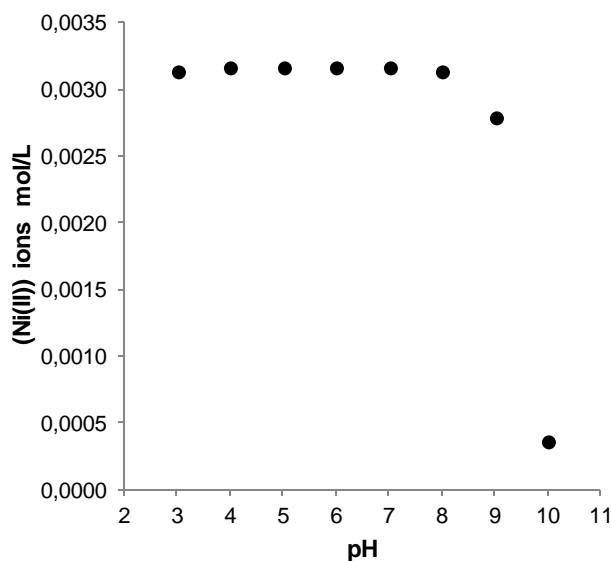


Figure 4. Nickel ions concentration decreases due to $Ni(OH)_2$ precipitation.

III.3. Effect of pH

The pH of solution greatly influences metal sorption due to the influence of pH on the deprotonation of functional groups. As can be seen from Figure. 5, the amount of Ni(II) adsorption on fungal biomass increased with the increase of pH from 2.0 to 8.0. At pH values above 8.0, nickel mainly precipitated as $Ni(OH)_2$ according to Visual MINTEQ. Therefore, the observed removal was attributed to precipitation and not to adsorption. At low pH, the cell wall ligands are closely associated with the hydronium ions and restrict the biosorption of Ni(II). As the pH increases, the hydronium ions are gradually dissociated and more active sites with negative charges such as carboxyl, phosphate, imidazole and amino groups would be available for the binding of Ni(II) as was confirmed by the study of pH_{zpc} . The maximum adsorption at pH 8.0 is due to the optimum combination between the functional groups on the biomass surface and ionic species of Ni(II). The following experiments were carried out at this pH value.

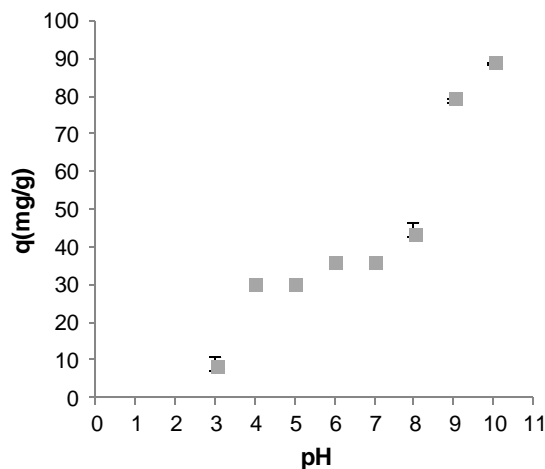


Figure 5. Effect of pH on the biosorption of Ni(II): $C_0=300$ mg/L, particle size 100-200 μm , and contact time = 3h.

III.4. Effect of initial metal concentration

The effect of initial nickel concentration on adsorption of nickel ions at pH 8.0 is shown in figure. 6. The amount of nickel adsorption by fungal biomass increased rapidly when initial metal concentration was increased from 50 to 500 mg/L. The maximum biosorption capacity of *Pleurotus mutilus* achieved at an initial Ni(II) concentration of 478.995 mg/L was 47.101 mg/g. After the equilibrium, the removal of nickel ions was not significant due to the limited adsorption sites and electrostatic repulsion on the surface.

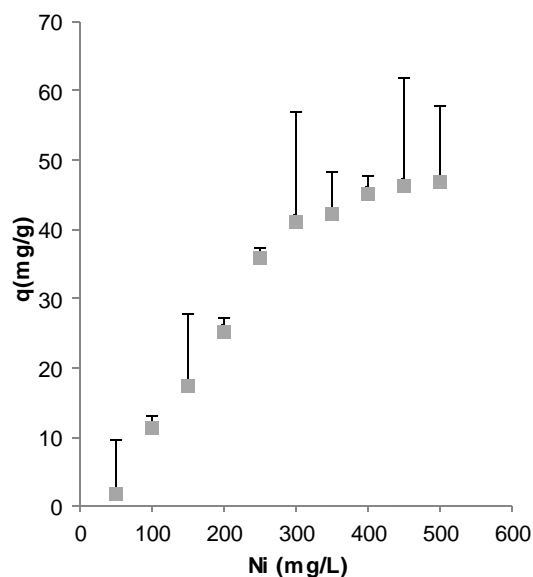


Figure 6. Effect of Initial metal concentration on the biosorption of Ni(II): pH 8.0, particle size 100-200 μm , and contact time = 3h.

III. 5.Effect of contact time

Contact time is one of the key parameters for successful biosorption application. The effect of contact time on biosorption of Ni(II) is depicted on figure. 7. The sorption rate of Ni(II) was initially high and decreased with an increase in contact time. The initial fast uptake is probably due to the high initial Ni(II) concentration and empty metal binding sites on fungal biomass. Whereas the rate of biosorption decreases due to the saturation of metal binding sites. The equilibrium was reached within 79 min. An additional increase in contact time had a slight effect on the amount of biosorption.

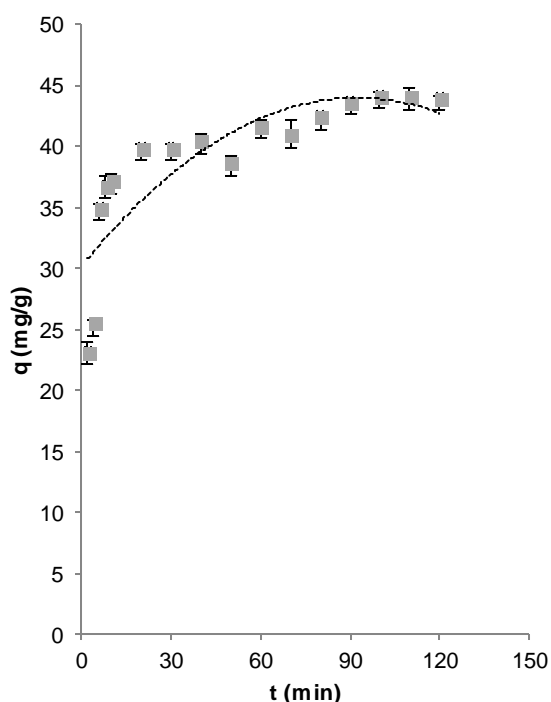


Figure 7. Effect of contact time on the biosorption of Ni(II): pH 8.0, $C_0 = 300$ mg/L and particle size 100-200 μm .

III.6.Effect of particle size on nickel biosorption

The influence of particle size of *Pleurotusmutilus* on nickel biosorption is reported in figure. 8. *Pleurotusmutilus* removed more nickel ions (48.539 mg/g) with particle size ranging from 200 μm to 300 μm . The effect of *Pleurotusmutilus* particle size was not significant (P-value= 0.364 > 0.05).

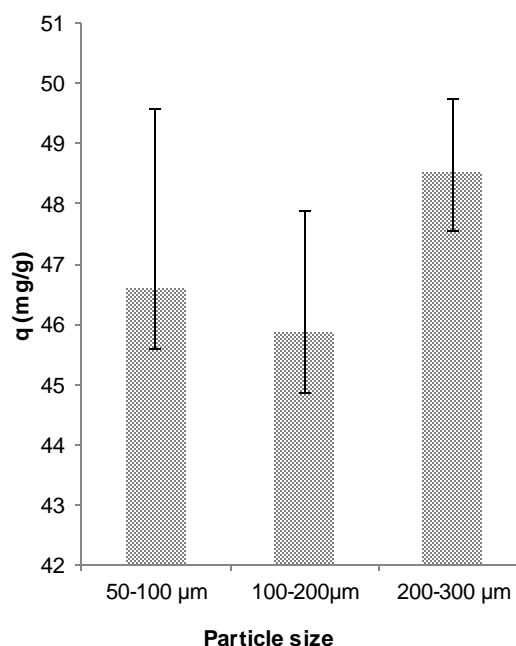


Figure 8. Effect of particle size on the biosorption of Ni(II): pH 8.0, $C_0 = 300$ mg/L, and contact time = 3h.

III.7.Biosorption isotherms

The values of Langmuir, Freundlich, Temkin and Dubinin-Radushkevich parameters are summarized in Table 3.

Table 3. Adsorption isotherm models parameters

Isotherm model	<i>Pleurotusmutilus</i>
Langmuir	
q_{max} (mg/g)	47.169
K_L (L/mg)	0.0042
R_L	0.606
R^2	0.688
Freundlich	
K_f (L/mg)	0.029
n	0.7452
R^2	0.792
Temkin	
a_T (L/mg)	0.026
b_T (J/mol)	104.849
R^2	0.950
Dubinin-Radushkevich	
q_D (mg/g)	47.153
B (mol^2/J^2)	-1.3×10^{-9}
E (J/mol)	196116.614
R^2	0.9836

III.7.1. Langmuir model

The Langmuir constant (K_L) and q_{max} are calculated from the slopes and intercepts of $1/q_e$ versus $1/C_e$ respectively (figure. 9). The predicted q_{max} of Ni(II) biosorption capacities of *Pleurotusmutilus* was 47.169 mg/g. The separation factor R_L indicated that the biosorption for Ni(II) was favorable.

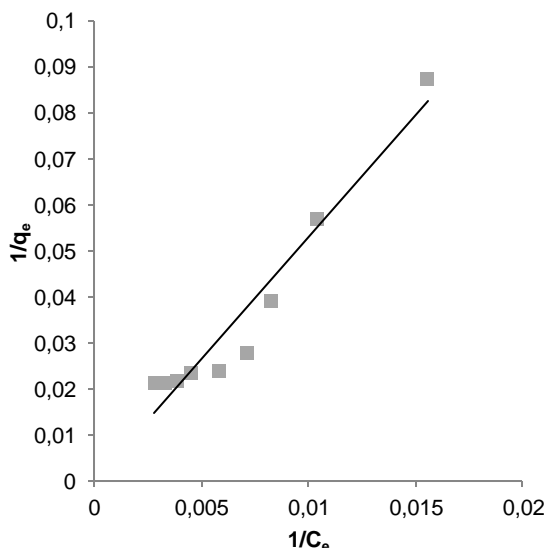


Figure 9. The linear form of Langmuir adsorption isotherm of Ni(II).

III.7.2. Freundlich model

The Freundlich isotherm for the adsorption of nickel on *Pleurotusmutilus* presented in figure. 10. The values of K_f and $1/n$ are calculated from the intercepts and slopes respectively. The value of heterogeneity factor “n” are greater than unity, indicating that Ni(II) ions are favorably adsorbed (table 3).

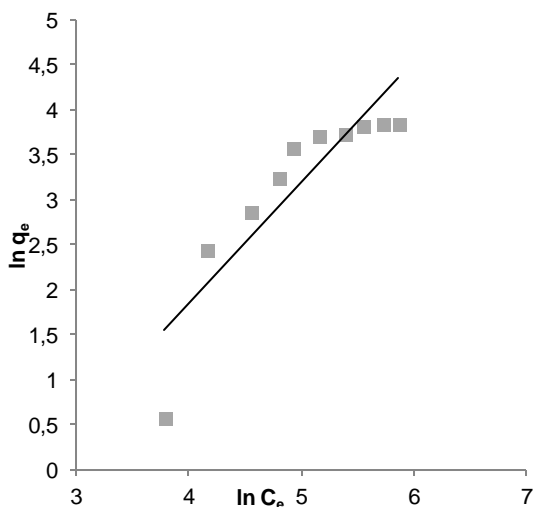


Figure 10. The linear form of the Freundlich adsorption isotherm equation for Ni(II).

III.7.3. Temkin model

The Temkin constants a_T and b_T are calculated from the slopes and intercepts of q_e vs $\ln C_e$ respectively (figure 11). Typical bonding energy range for ion-exchange mechanism is reported to be in the range of 8000-16000 J/mol while physisorption processes are reported to have adsorption energies less than -40000 J/mol. Very low value of b_T (86.949 J/mol) obtained in the present study indicates that the adsorption process involves both chemisorption and physisorption [47, 48].

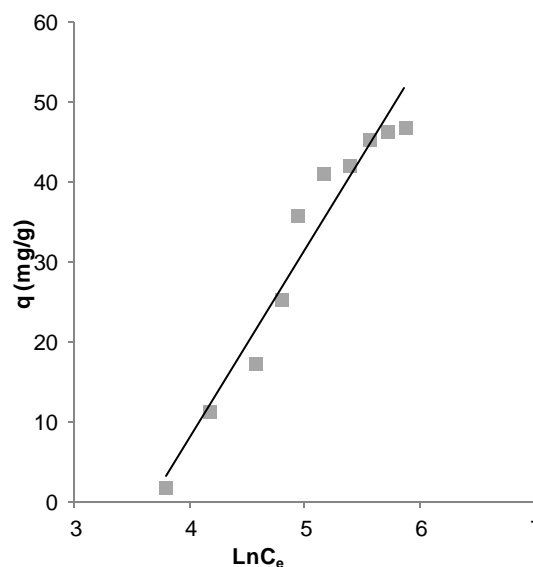


Figure 11. Temkin adsorption isotherm for Ni(II).

III.7.4. The Dubinin-Radushkevich (D-R)

The Dubinin-Radushkevich constants and mean free energy are given in Table 3. The constants q_D and B are calculated from the slope and intercept respectively (figure. 12). The value of the mean biosorption energy (E) suggests that the biosorption process of nickel ions onto *Pleurotusmutilus* dominated by particle diffusion.

A comparison of the R^2 values for models suggested that the Dubinin-Radushkevich fitted the data best followed by the Temkin isotherms.

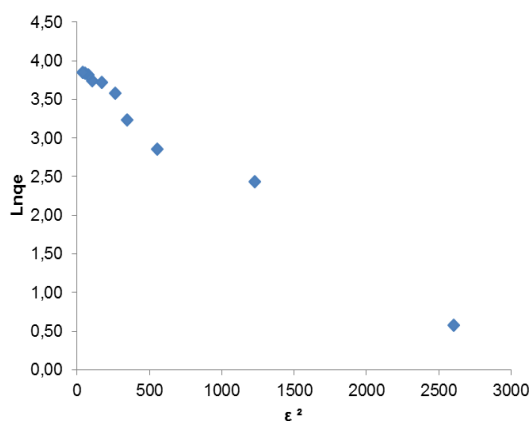


Figure 12. Dubinin-Radushkevich adsorption isotherm for Ni(II).

III.8. Biosorption kinetic models

The kinetic data were analyzed using various kinetic models: pseudo-first-order model, pseudo-second-order model, Elovitch model, Intra-particle diffusion model and Boyd model.

Kinetic parameters are presented in Table 4. The higher values of R² and the accuracy to predict q_{eq} were used as criteria to define the most suitable model to describe sorption kinetics of Ni(II).

Table 4. Comparison of kinetic parameters for adsorption of Ni(II) by *Pleurotus mutilus*.

Kinetic model	<i>Pleurotus mutilus</i>
Pseudo-first-order	
q _{e,exp} (mg/g)	44.022
q _{e,calc} (mg/g)	7.243
k ₁ (1/min)	0.041
R ²	0.448
Pseudo-second-order	
q _{e,exp} (mg/g)	44.022
q _{e,calc} (mg/g)	43.478
k ₂ (g/mg min)	0.016
h (mg/g min))	30.303
t ^{1/2} (min)	1.435
R ²	0.998
Elovich	
α (mg/g min)	6711.670
β (g/mg)	0.278
R ²	0.848
Intraparticle diffusion	
K _p (mg/g min ^{1/2})	0.322
C (mg/g)	30.966
R ²	0.686
Boyd model	
K _{fd} (min ⁻¹)	24.927
R ²	0.448

III.8.1. Pseudo-first-order kinetic model

Straight-line plot of log (q_e - q_t) against t was used to determine the rate constant k₁ and correlation coefficients R² (Figure. 13). The intercept of the plot should be equal to log q_{eq}. However, if calculated q_{eq} does not equal the equilibrium metal uptake then the reaction is not likely to be first order even if this equation has a high correlation with the experimental data [27, 49]. The calculated q_{eq} is not close to experimental q_{eq} (table 4) suggesting the insufficiency of the pseudo-first-order model to fit the kinetic data.

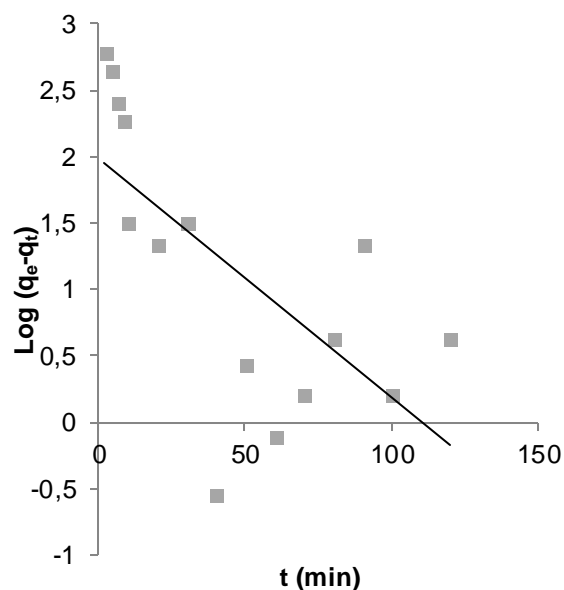


Figure 13. Pseudo-first-order kinetics of Ni(II).

III.8.2. Pseudo-second-order model

A pseudo-second-order model proposed by Ho and McKay [34] was then used to explain the sorption kinetics (figure. 14). The rate constant and the correlation coefficient are also summarized in Table 4. The correlation coefficient R² for the pseudo-second-order adsorption model has very high value (0.998). Besides, the adsorption capacity calculated by the pseudo-second-order model is also close to that determined by experiments. Therefore, it has been concluded that the pseudo-second-order adsorption model is more suitable to describe the adsorption kinetics. This result suggests that the biosorption of Ni(II) onto *Pleurotus mutilus* is likely to be a chemisorption process involving exchange or sharing of electrons mainly between metal ions and functional groups of the biosorbent [49].

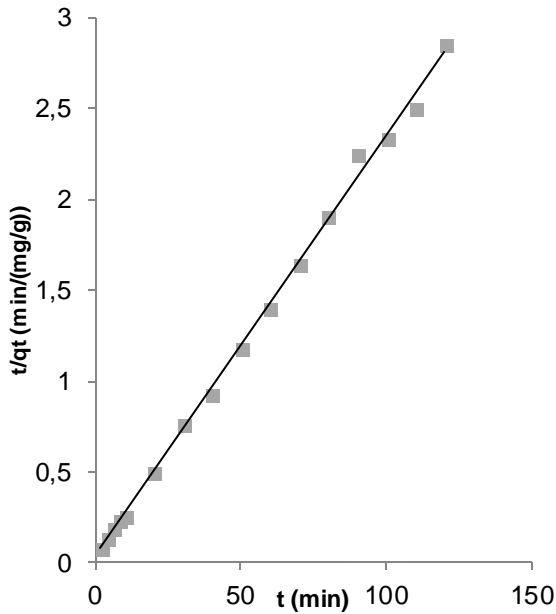


Figure 14. Pseudo-second-order kinetics of Ni(II).

III.8.3. Elovich model

The plot of q_t versus $\ln t$ for the Elovich equation is shown in figure. 15. The parameters of the Elovich equation are shown in Table 4.

Elovich equation agreed well with the experimental values ($R^2 > 0.84$). This confirms that the adsorption of nickel by *Pleurotusmutilus* is controlled by chemisorption process.

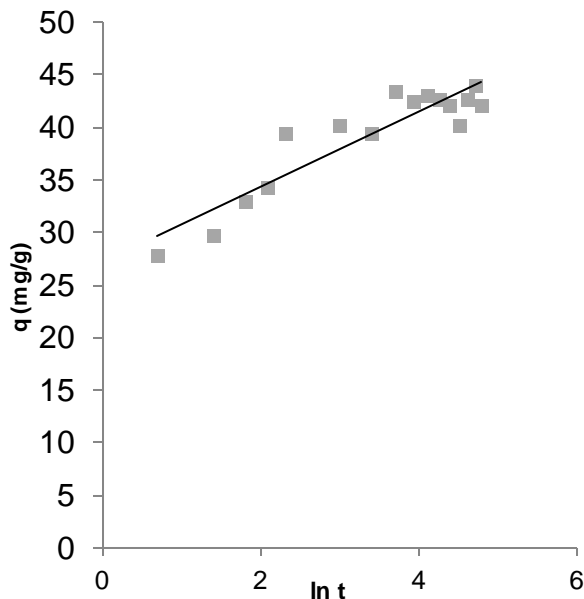


Figure 15. Elovich kinetics for Ni(II) adsorption.

III. 8.4. Intra-particle diffusion model

The experimental data were fitted to Weber and Morris model to evaluate whether intraparticle diffusion controlled the rate of Ni(II) adsorption. The plots of q_t versus $t^{1/2}$ showed that the straight line did not pass through the origin (Figure. 16). This suggested that the intraparticle diffusion effect was not the rate-controlling mechanism of the biosorption process. Based on this plot, the biosorption process of the Ni(II) entails two phases, the initial portion of the plot indicated an external mass transfer across the liquid film whereas the second linear portion is due to intraparticle or pore diffusion but was not the rate-limiting step. Similar results were reported by Sahmoun et al. (2009) [50] for the adsorption of Cr(III) by *Streptomyces rimosus* and by Chergui et al. (2009) [11] for the adsorption of hexacyanoferrate(III) by *Pleurotusmutilus*.

The slope of the second linear portion of the plot has been identified as the intraparticle diffusion rate constant (K_p) [50]. The values of C and K_p are given in Table 4.

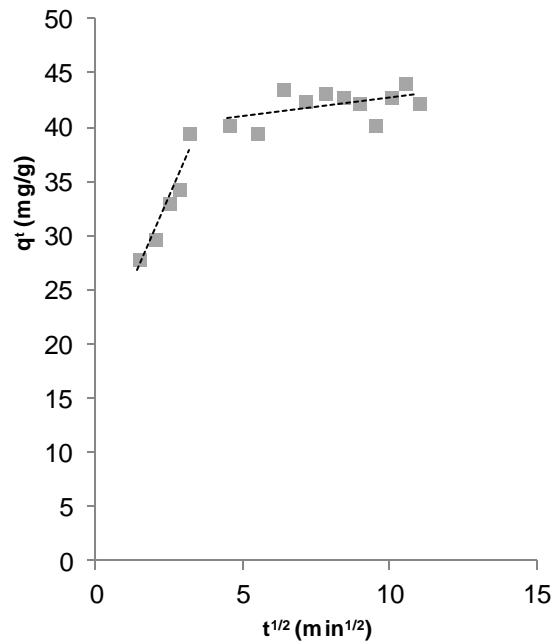


Figure 16. Intraparticle diffusion plot sorption of Ni(II).

III.8.5. Boyd model

The Boyd plot was obtained by plotting B_t versus time (Figure. 17). The plot was neither linear nor pass through the origin with low correlation coefficients (table 4). This suggested that the film diffusion is the rate limiting mechanism in Ni(II) biosorption by *Pleurotusmutilus*.

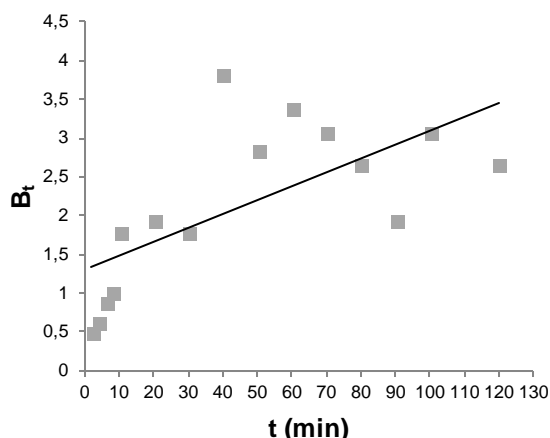


Figure 17. Boyd plot for the biosorption of Ni(II).

While six kinetic models were fitted to the experimental data, only the pseudo-second-order model fit the sorption kinetics well with a correlation coefficient of 0.998. This adsorption kinetic is typical for the adsorption of divalent metals onto biosorbents [51].

III.9. Thermodynamics of biosorption

The values of ΔG^0 are summarized in table 5. The change in the standard free energy has negative value for the whole range of concentration. These results indicate that the adsorption of Ni(II) by *Pleurotusmutilus* was spontaneous and thermodynamically favorable.

Table 5. Thermodynamic parameters of free energy of adsorption ΔG^0 .

Ni (mg/l)	ΔG^0 (kJ/mol)
50.00	-7.92
100.00	-1.44
150.00	-1.42
200.00	-1.06
250.00	-0.57
300.00	-0.75
350.00	-1.27
400.00	-1.50
450.00	-1.84
500.00	-2.16

IV. Conclusion

The current study shows that the fungal biomass of *Pleurotus mutilus* is effective biosorbent for the removal of Ni(II) from aqueous solution. The speciation model predicted the formation of nickel precipitates at pH above 8.0. The biosorption

performance was strongly affected by solution pH and contact time at room temperature. The optimum pH for biosorption of Ni(II) on *Pleurotus mutilus* was achieved at pH 8.0. Nickel biosorption by *Pleurotus mutilus* was fitted well with Dubinin-Radushkevich and Temkin isotherms equations within the investigated metal concentration range. The maximum adsorption capacities (q_{max}) calculated from Langmuir adsorption isotherm was 47.169 mg/g. The kinetics of the biosorption of Ni(II) was better described with pseudo-second-order kinetics. The negative values of ΔG^0 indicate spontaneous adsorption of nickel. The results obtained through this study support that filamentous fungi is effective and low cost biosorbent for Ni(II) removal from aqueous solutions.

V. References

- Zafar, M.N.; Aslam, I.; Nadeem, R.; Munir, S.; Rana, U.A.; Khan, S.U.D. Characterization of chemically modified biosorbents from rice bran for biosorption of Ni(II). *Journal of Taiwan Institute of Chemical Engineering* 46 (2015) 82-88.
- Lam, Y.F.; Lee, L.Y.; Chua, S.J.; Lim, S.S.; Gan, S. Insights into the equilibrium, kinetic and thermodynamics of nickel removal by environmental friendly *Lansium domesticum* peel biosorbent. *Ecotoxicological Environment Safety* 127 (2016)61-70.
- Çelekli, A.; Bozkurt, H. Biosorption of cadmium and nickel ions using *Spirulina platensis*: Kinetic and equilibrium studies. *Desalination* 275 (2011)141-147.
- Coman, V.; Robotin, B.; Ilea, P. Nickel recovery/removal from industrial wastes: A review. *Resource Conservation Recycling* 73 (2013)229-238.
- Abdolali, A.; Ngo, H.H.; Guo, W.; Lu, S.; Chen, S.; Nguyen, N.C.; Zhang, X.; Wang, J.; Wu, Y. A breakthrough biosorbent in removing heavy metals: Equilibrium, kinetic, thermodynamic and mechanism analyses in a lab-scale study. *Science Total Environment* 542 (2016) 603-611.
- Shinde, N.R.; Bankar, A. V.; Kumar, A.R.; Zinjarde, S.S. Removal of Ni(II) ions from aqueous solutions by biosorption onto two strains of *Yarrowialipolytica*. *Journal of Environmental. Management* 102 (2012) 115-124.
- Alam, M.Z.; Ahmad, S.; Azhar, E.I.; Haque, A.; Alam, Q. Microbial sorption and desorption of chromium, cadmium and nickel from aqueous solution by dried and non growing biomasses of *Staphylococcus gallinarum* W-61. *Journal of Pure Applied Microbiology* 8 (2014) 1961-1972.
- Amin, F.; Talpur, F.; Balouch, A.; Surhio, M.; Bhutto, M. Biosorption of fluoride from aqueous solution by white- rot fungus *Pleurotuserynгии* ATCC 90888. *Environmental Nanotechnology. Monitoring & Management* 3 (2014) 30-37.
- Sivaprakash, K.; Blessi, A.T.L.; Madhavan, J. Biosorption of nickel from industrial wastewater using *Zygnema sp.* *Journal of Institute Engineering* 96 (2015) 319-326.
- Sheng, P.X.; Ting, Y.P.; Chen, J.P.; Hong L. Sorption of lead, copper, cadmium, zinc, and nickel by marine algal biomass: characterization of biosorptive capacity and investigation of mechanisms. *Journal of Colloid and Interface Science* 275 (2004) 131-141.
- Chergui, A.; Kerbachi, R.; Junter, G.A. Biosorption of hexacyanoferrate(III) complex anion to dead biomass of the basidiomycete *Pleurotusmutilus*: Biosorbent

- characterization and batch experiments. *Chemical Engineering Journal* 147 (2009) 150-160.
12. Henini, G.; Laidani, Y.; Souahi, F. Study of adsorption of copper on biomass *Pleurotusmutilus* and the possibility of its regeneration by desorption. *Energy Procedia* 6 (2011) 44-448.
 13. Moussous, S.; Selatnia, A.; Merati, A.; Junter, G.A.: Batch cadmium (II) biosorption by an industrial residue of macrofungal biomass (*Clitopiluscyphoides*). *Chemical Engineering Journal* 197 (2012) 261–271.
 14. Yeddou-Mezenner, N. Kinetics and mechanism of dye biosorption onto an untreated antibiotic waste. *Desalination* 262 (2010) 251–259.
 15. Behloul, M.; Lounici, H.; Abdi, N.; Drouiche, N.; Mameri, N.. Adsorption study of metribuzin pesticide on fungus *Pleurotusmutilus*. *International. Biodeterioration and Biodegradation*.1 (2016) 1-9.
 16. Gorgievski, M.; Bozic, D.; Stankovic, V.; Strbac, N.; Serbula, S. Kinetics, equilibrium and mechanism of Cu^{2+} , Ni^{2+} and Zn^{2+} ions biosorption using wheat straw. *Ecological. Engineering* 58 (2013) 113-122.
 17. Blanes, P.S.; Bordoni, M.E.; González, J.C.; García, S.I.; Atria, A.M.; Sala, L.F.; Bellú, S. E. Application of soy hull biomass in removal of Cr(VI) from contaminated waters. Kinetic, thermodynamic and continuous sorption studies. *Journal of Environmental Chemical Engineering* 4 (2016) 516-526.
 18. Boehm, H.P. Some aspects of the surface chemistry of carbon blacks and other carbons. *Carbon* 32 (1994) 759-769.
 19. Hackbarth F.V.; Girardi, F.; De Souza, S.M.A.G.U.; De Souza, A.A.U.; Boaventura, R.A.R.; Vilar, V.J.P. Marine macroalgae *Pelvetiacauniculata* (*Phaeophyceae*) as a natural cation exchanger for cadmium and lead ions separation in aqueous solutions. *Chemical. Engineering Journal* 242(2014) 294-305.
 20. Kapetas, L.; Ngwenya, B.T.; Macdonald, A.M.; Elphick, S.C. Kinetics of bacterial potentiometric titrations: the effect of equilibration time on buffering capacity of *Pantoeaagglomerans* suspensions. *Journal of Colloid Interface Science*. 359 (2011) 481-486.
 21. Cazón, J.P.; Viera, M.; Donati, E.; Guibal, E. Zinc and cadmium removal by biosorption on *Undariapinnatifida* in batch and continuous processes. *Journal of Environmental Management* 129 (2013) 423-434.
 22. Gray-Munro, J.E.; and Strong, M. A study on the interfacial chemistry of magnesium hydroxide surfaces in aqueous phosphate solutions: Influence of Ca^{2+} , Cl and protein. *Journal of Colloid Interface Science* 393 (2013) 421-428.
 23. Mishra, A.; Tripathi, B.D.; Raib, A.K. Biosorption of Cr(VI) and Ni(II) onto *Hydrilla verticillata* dried biomass. *Ecological Engineering* 73 (2014) 713-723.
 24. Kirova, G.; Velkova, Z.; Stoytcheva, M.; Hristova, Y.; Iliev, I.; Gochev, V. Biosorption of Pb(II) ions from aqueous solutions by waste biomass of *Streptomyces fradiae* pretreated with NaOH. *Biotechnology and Biotechnological Equipment* 29 (2015) 689-695.
 25. Selatnia, A.; Madani, A.; Bakhti, M.Z.; Kertous, L.; Mansouri, Y.; Yous R. Biosorption of Ni^{2+} from aqueous solution by a NaOH-treated bacterial dead *Streptomyces rimosus* biomass. *Mineral Engineering* 17 (2004) 903-911.
 26. Zhu, W.; Xu, X.; Xia, L.; Huang, Q.; Chen, W. Comparative analysis of mechanisms of Cd^{2+} and Ni^{2+} biosorption by living and nonliving *Mucoromycote* sp. XLC. *Geomicrobiology Journal* 33 (2016) 274-282.
 27. Joo, J.H.; Hassan, S.H.A.; Oh, S.E. Comparative study of biosorption of Zn^{2+} by *Pseudomonas aeruginosa* and *Bacillus cereus*. *International Biodeterioration and Biodegradation* 64 (2010) 734-741.
 28. Martins, A.C.; Pezotia, O.; Cazetta, A.L.; Bedin, K.C.; Yamazaki, D.A.S.; Bandoch, G.F.G.; Asefa, T.; Visentainer, J.V.; Almeida, V.C. Removal of tetracycline by NaOH-activated carbon produced from macadamia nut shells: Kinetic and equilibrium studies. *Chemical. Engineering Journal* 260 (2015) 291-299.
 29. Vijayaraghavan, K.; Padmesh, T. V.N.; Palanivelu, K.; Velan, M. Biosorption of nickel (II) ions onto *Sargassum wightii*: Application of two-parameter and three-parameter isotherm models. *Journal of Hazardous Material* B133 (2006) 304-308.
 30. Sivakumar P.; and Palanisamy, P.N. Adsorption studies of basic red 29 by a non-conventional activated carbon prepared from *euphorbia antiquorum* L. *International Journal of Chemical Technology and Research* 1 (2009) 502-510.
 31. Barka, N.; Ouzaouit, K.; Abdennouri, M.; El Makhfouk, M. Dried prickly pear cactus (*Opuntia ficus indica*) cladodes as a low-cost and eco-friendly biosorbent for dyes removal from aqueous solution. *Journal of Taiwan Institute of Chemical Engineering* 44 (2013) 52-60.
 32. Osasona, I.; Faboya, O.L.; Oso, A.O. Kinetic, equilibrium and thermodynamic studies of the adsorption of methylene blue from synthetic wastewater using cow hooves. *Braslian Journal of Applied Science and Technology* 3 (2013) 1006-1021.
 33. Lagergren, S. Ueber die Dämpfung electrischer resonatoren. *Annals of Physics (Berlin, Ger.)* 300 (1898) 193-416. 34. Ho, Y.S.; McKay, G. Pseudo-second order model for sorption processes. *Process Biochemistry* 34 (1999) 451-465.
 35. Bayramoglu, G.; Akbulut, A.; Arica, M.Y. Aminopyridine modified *Spirulina platensis* biomass for chromium(VI) adsorption in aqueous solution. *Water Science and Technology* 74 (2016), 914-926.
 36. Weber W.J.; Morris, J.C. Intraparticle diffusion during the sorption of surfactants onto activated carbon. *Journal of Sanitary Engineering. Division* 89 (1963) 53- 61.
 37. Boyd, G.E.; Adamson, A.W.; Myers, L.S. The exchange adsorption of ions from aqueous solutions by organic zeolites. *Journal of American. Chemistry Society* 69 (1947) 2836-2848.
 38. Das, D.; Varghese, L.R.; Das, N. Enhanced TDS removal using cyclodextrinated, sulfonated and aminated forms of bead-membrane duo nanobiocomposite via sophorolipid mediated complexation. *Desalination* 360 (2015) 35-44.
 39. Nethaji, S.; Sivasamy, A.; Thennarasu, G.; Saravanan, S. Adsorption of malachite green dye onto activated carbon derived from *Borassusaethiopicum* flower biomass. *Journal of Hazardous Material* 181 (2010) 271-280.
 40. Ofudje, E.A.; Akiode, O.K.; Oladipo, G.O.; Adedapo, A.E.; Adebayo, L.O.; Awotula, A.O. Application of raw and alkaline-modified coconut shaft as a biosorbent for Pb^{2+} removal. *Bioresources Technology* 10 (2015) 3462-3480.
 41. Leyva-Ramos, R.; Bernal-Jacome, L.A.; Acosta-Rodriguez, I. Adsorption of cadmium (II) from aqueous solution on natural and oxidized corncob. *Separation and Purification Technology* 45 (2005) 41-49.
 42. Dmytryk, A.; Saeid, A.; Chojnacka, K. Biosorption of microelements by *Spirulina*: towards technology of

- mineral feed supplements. *The Scientific World Journal* (2014).
43. Volesky, B. Biosorption and me, *Water Research* 41 (2007) 4017-4029.
 44. Ramrakhiani, L.;Majumder, R.; Khowala, S. Removal of hexavalent chromium by heat inactivated fungal biomass of *Termitomycesclypeatus*: Surface characterization and mechanism of biosorption, *Chemical Engineering Journal* 171(2011)1060-1068.
 45. Young, S.D.; Bache, B.W.; Welch, D.; Anderson, H.A. Analysis of the potentiometric titration of natural and synthetic polycarboxylates. *Journal of Soil Science* 32 (1981) 579-592.
 46. Michalak, I.; Chojnacka, K. Interactions of metal cations with anionic groups on the cell wall of the macroalga *Vaucheria* sp. *Engineering Life Science* 10 (2010) 209-217.
 47. Hu, X.J.; Wang, J.S.; Liu, Y.G.; Li, X.; Zeng, G.M.; Bao, Z.L.; Zeng, X.X.; Chen, A.W.; Long, F. Adsorption of chromium (VI) by ethylenediamine-modified cross-linked magnetic chitosan resin: isotherms, kinetics and thermodynamics. *Journal of Hazardous Material* 185 (2011) 306-314.
 48. Wang, W.Q.; Li, M.Y.; Zeng, Q.X. Thermodynamics of Cr(VI) adsorption on strong alkaline anion exchange fiber. *Transactions Nonferrous Material Society of China* 22 (2012) 2831-2839.
 49. Barka, N.; Abdennouri, M.; Boussaoud, A.; EL Makhfouk, M. Biosorption characteristics of cadmium(II) onto *Scolymushispanicus* L. as Low-Cost Natural Biosorbent. *Desalination* 258 (2010) 66-71.
 50. Sahmoune, M.N.; Louhab, K.; Boukhar, A. Biosorption of Cr(III) from Aqueous Solutions Using Bacterium Biomass *Streptomyces rimosus*. *International Journal of Environmental Research* 3 (2009) 229-238.
 51. Salvadori, M.R.; Ando, R.A.; Oller do Nascimento, C.A.; Corrêa, B. Intracellular Biosynthesis and Removal of Copper Nanoparticles by Dead Biomass of Yeast Isolated from the Wastewater of a Mine in the Brazilian Amazonia. *PLOS ONE* 9 (2014) 1-8.

Please cite this Article as:

Daoud N., Selatnia A., Benyoussef E.H., Nickel removal from aqueous solution by non-living *Pleurotus mutilus*: kinetic, equilibrium, and thermodynamic studies, ***Algerian J. Env. Sc. Technology*, 4:3 (2018) 30-43**